The Astrophysical Journal, Vol. **155**, March 1969

THE CORONAL BRIGHTNESS AT 2.23 MICRONS

Alan W. Peterson
Department of Physics and Astronomy, University of New Mexico, Albuquerque
Received June 27, 1968

ABSTRACT

Infrared observations of the corona during the November 12, 1966, eclipse reveal the presence of a sharp, thermal-emission zone at 3.9 $R_\odot$ where calculations predict interplanetary dust is undergoing rapid vaporization. A rounded emission zone with no sharp inner edge appears at 3.3 $R_\odot$ where, presumably, dust in elliptical orbits is undergoing less rapid vaporization. These observations add a new component to the coronal radiation field, i.e , interplanetary dust emission. The thermal emission is found to contribute to coronal reddening but, in addition, it is found that diffraction must also contribute to the observed reddening. Sufficient spectral data are not yet available to specify the dust-vaporization temperature more precisely than earlier estimates of 800°–2000° K.

I. INTRODUCTION

Infrared observations of the total eclipse of November 12, 1966, were made in an attempt (1) to observe the predicted infrared peak and cutoff at the edge of the dust-free zone which surrounds the Sun (Peterson 1963), (2) to redetermine the infrared excess as observed by Blackwell (1952) at the eclipse of 1952, (3) to extend the measurements of coronal reddening over a larger angular range, (4) to determine the role of dust emission in coronal reddening, and (5) to study the infrared excess and the size of the dust-free zone in order to obtain information about the size and chemical composition of interplanetary dust. Preliminary results relating primarily to the detection of dust emission have already been presented (Peterson and MacQueen 1967; Peterson 1967*a*). In the present paper we discuss the remaining topics.

II. OBSERVATIONS

The observations were performed at Huachacalla, Bolivia, at an altitude of over 13000 feet. A simple 6-inch, f/4, reflecting telescope focused radiation through an interference filter and dry-ice cooled chopper onto a 1-mm-square selected PbS detector which was also cooled by dry ice. The resulting signal was amplified, rectified with a phase-sensitive system, and recorded on a strip chart. The detector's square field of view was 5′.6, or 0.35 $R_\odot$, on each side.

During totality three scans of the corona were planned. Each was to extend from 4° above the Sun to 2° below the Sun along a vertical circle. One scan was lost, and the remaining two scans were made at 2.23 μ (band pass 0.42 μ) so as to record the entire range of coronal brightness. During the 30 seconds after totality the telescope was shifted 0°.75 in azimuth to the north and an additional scan was recorded of the corona and of the brightening sky at 3.53 μ (band pass 0.32 μ).

The weather before, during, and after totality was marred by light to moderate cirrus clouds covering most of the sky. However, no visual impression of the presence of these clouds was obtained when the sky and corona were viewed through a finder telescope during one coronal scan at totality. The path of the scans coincided roughly with the ecliptic; the exact path is shown in Figure 1.

Prior to the eclipse both absolute and relative calibrations were performed. At the eclipse site only relative calibrations, provided by viewing the Sun directly through an aperture stop of 0.044-inch diameter, were made. The absolute calibrations were made with a full-aperture, blackened-cone source heated with stirred boiling water. Later, a high-temperature black body was obtained, and new calibrations were made at source temperatures of 600°, 800°, and 1000° K. These furnished calibration charts with a range of input power to the detector of over four decades. We believe the latter calibrations to be superior to the earlier single-point calibrations, and they are used in the reductions to be presented. For the sake of completeness we present an intercomparison of the three calibrations in Table 1. The conversion to relative brightness in terms of the mean solar disk was made by using Johnson's (1954) values for the spectral-energy distribution of the Sun.

III. RESULTS

a) The Coronal Brightness

In Figure 2 we present the absolute coronal-intensity distribution at 2.23 μ. Three components of coronal radiation are distinguishable by their characteristic angular dependence. First, the K-component dominates from the Sun's limb out to 1.75 $R_\odot$ to the west and 2.0 $R_\odot$ to the east. The inner corona is less bright to the west of the Sun; this is also revealed by direct photographs and by the fact that the scan did not cross the large plume extending to the southwest. Second, the F-component emerges and extends out to 3 $R_\odot$. Third, the predicted thermal emission, the T-component, appears in two regions: as a rounded bump with a maximum near 3.3 $R_\odot$ and a sharp peak at 3.9 $R_\odot$. This latter peak was the behavior predicted by calculations (Peterson 1963); however, the rounded bump requires a new interpretation given in § III*b*. Finally, beyond

TABLE 1

COMPARISON OF CALIBRATIONS FOR 1 MV OUTPUT

Source	Equivalent Brightness ($B_\odot$) 2.23 μ	3 53 μ
Aperture stop.	1 23$\times10^{-7}$	2.75$\times10^{-6}$
Cone... .. .	6 05$\times10^{-8}$	2 00$\times10^{-6}$
Black body.	1 57$\times10^{-7}$	1 39$\times10^{-6}$

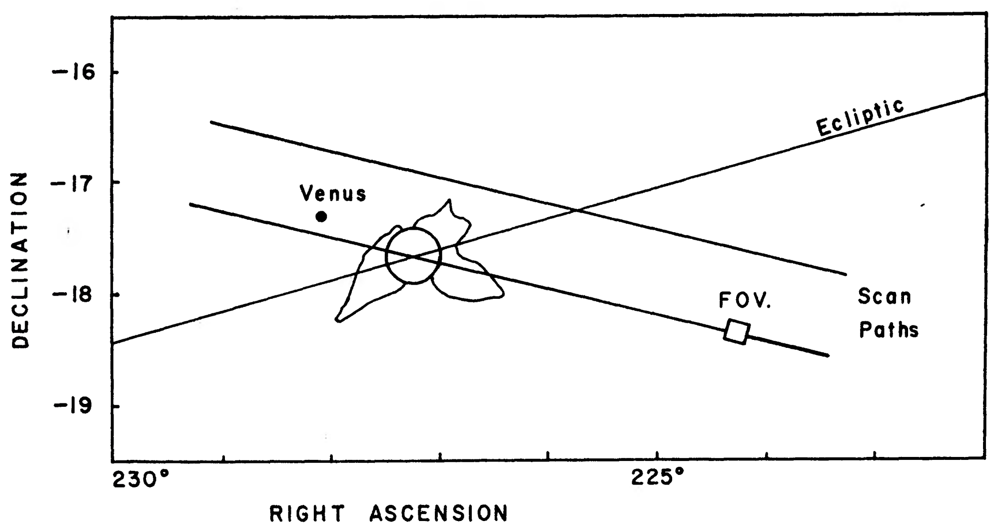

FIG. 1.—Field of view (*F.O.V.*) and scanning paths across the corona for two scans at 2.23 μ. The scan at 3.53 μ was displaced 0°.75 to the north.

4.5 $R_\odot$ the F-component reappears and continues to the point where the signal merges with the fluctuations near zero scale reading.

The inner K-coronal brightness falls below the usual exponential value for elongations less than 1.35 $R_\odot$ because a portion of the detector then views the Moon. Between 1.25 and 1.75 $R_\odot$ the measured brightness and slope of the angular distribution may be compared with other measurements. Table 2 gives the coronal brightness to the east and west of the Sun at 1.5 $R_\odot$ and the slope of the K-component distribution between 1.3 and 1.9 $R_\odot$. Ingham's (1961) corona compilation values are entered for comparison.

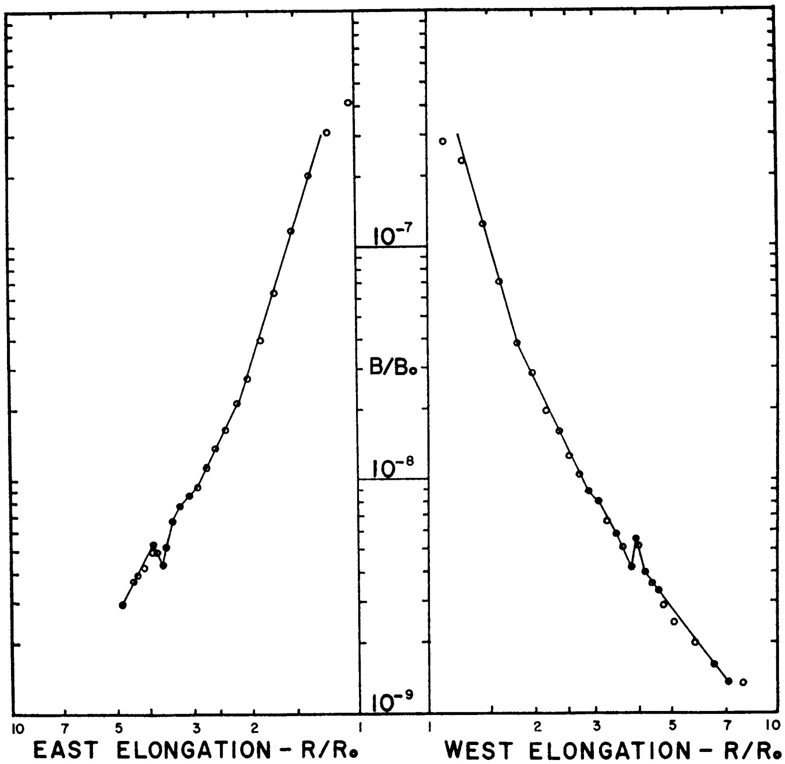

FIG. 2.—Distribution of coronal brightness at 2.23 μ. Thermal-emission zones, due to interplanetary dust approaching the Sun, appear at 3.3 and 3.9 $R_\odot$. Peaks at 3.9 $R_\odot$ are interpreted as due to complete vaporization of the dust in circular orbits while peaks at 3.3 $R_\odot$ presumably are due to particles, not vaporizing completely, and moving in elliptical orbits. Straight-line segments approximately delineate the K- and F-components in the inner corona. Near the limb the detector views the dark Moon, and the signal falls below the exponential value.

Between 2.0 and 3.0 $R_\odot$ the measured values referring primarily to the F-component may again be compared with Ingham's. Here the corona is becoming brighter in the infrared, and the slope of the brightness distribution is less than in visible light.

b) The Thermal-Emission Zones

The presence of two regions of thermal emission with dissimilar angular distribution was not expected on the basis of earlier calculations (Peterson 1963) which assumed that all dust particles were of the same chemical composition, and that they moved in circular orbits. With dust of differing chemical composition and thus different vaporization temperatures thermal-emission zones with sharp inner edges should be present at various distances from the Sun (Peterson 1964). Hence, we readily understand the sharp peak at 3.9 $R_\odot$ as being due to dust of a chemically homogeneous nature which is vaporizing completely while approaching the Sun in near-circular orbits due to the action of the

Poynting-Robertson effect and other drag forces. The relatively high intensity values between 3.0 and 3.8 $R_\odot$ show no sharp inner edge. We conclude that complete vaporization of the dust does not occur for this particle population. A reasonable interpretation of this emission zone is that the radiating dust particles are in elliptical orbits in which the particles sweep in close to the Sun, heat up, and radiate copiously, but do not remain in the vicinity of perihelion sufficiently long for complete vaporization to occur. If this interpretation is valid the radiation distribution will be directly related to the particle population's distribution of perihelion distances.

Beyond 4.5 $R_\odot$ the measured coronal brightness is considerably above the values measured in the visual range. We believe that several factors contribute to this excess brightness. A part may be due to an intrinsic reddening of the outer corona as others have found previously (Allen 1946; Blackwell 1952). Another part may be due to thermal emission of the dust before it reaches the rapid-vaporization zone. Finally, we must not overlook the possible increase in sky brightness caused by the cirrus clouds, although this is believed to be no larger than the fluctuations in brightness appearing in the outer portion of the western scan.

TABLE 2

CORONAL BRIGHTNESS AND GRADIENT COMPARED WITH INGHAM'S (1961) VALUES

r ($R_\odot$)	B ($B_\odot$)	Gradient
1 5		
West ..	1.03×10^{-7}	5.5
East.	$1\ 15\times10^{-7}$	6 3
Ingham .	1.20×10^{-7}	6 2
2 5		
West..... .	1.19×10^{-8}	3 1
East. . .	$1\ 46\times10^{-8}$	3 1
Ingham	$9\ 9\ \times10^{-9}$	3.4

An approximate separation of the thermal emission from the remainder of the corona is possible by extrapolating the F-component outward with its gradient the same as where no thermal emission appears. These values are given in Table 3 and are compared with our earlier calculations (Peterson 1963).

The lack of better agreement between the predicted and measured values can be attributed to several causes. First, the calculations used an emissivity for the dust based upon Ingham's (1961) evaluation of the zodiacal dust albedo; this emissivity may not apply to the real dust, particularly if emission bands are present; it may also be dependent upon distance from the Sun. Second, the calculations assume a dust density in space determined from Ingham's work, and that this dust density follows an $r^{-1\ 5}$ increase toward the Sun until complete vaporization occurs. This latter assumption is now known to be invalid because measurements from a balloon by MacQueen (1967) have revealed the presence of two additional vaporization zones at 8.7 and 9.25 $R_\odot$. Thus, some of the dust disappears before reaching 4 $R_\odot$.

c) Coronal Reddening

Data obtained on the inner corona have been used to investigate the infrared excess first measured by Blackwell (1952). The reddening coefficient defined by Blackwell is

$$R = \frac{B(\lambda_2,r_2)B(\lambda_1,r_1)}{B(\lambda_2,r_1)B(\lambda_1,r_2)} ,$$

where the $B(\lambda,r)$ refer to four brightness measurements made at two wavelengths (λ_1 and λ_2) and at two elongations (r_1 and r_2). If the coronal brightness changes with elongation in the same manner at each wavelength then $R = 1$ and the corona is of the same color as the photosphere. If $R > 1$ the corona is redder than the photosphere.

The values of R calculated from our data for λ_2, and the coronal-intensity distribution tabulated by Ingham for λ_1 gives the values plotted in Figure 3. In all cases $r_1 = 1.5\,R_\odot$ and at this point $R = 1$ because the light is due primarily to the K-corona. The abrupt increase in R at $3.9\,R_\odot$ is due to the dust-emission peak at that point. If the dust emission is removed from the coronal brightness we still find $R > 1$; the values corrected for dust emission are indicated in Figure 3 also. Now it appears that R attains a maximum

TABLE 3

COMPARISON OF MEASURED AND CALCULATED THERMAL EMISSION

r ($R_\odot$)	B ($B_\odot$)	B (W cm^{-2} sterad^{-1} μ^{-1})	Calculated (W cm^{-2} sterad^{-1} μ^{-1})
	Measured at 2.23 μ		
3 3			
West .	$9\ 2\ \times10^{-10}$	$9\ 9\times10^{-8}$	$2\ 2\times10^{-6}$
East.. ...	$1.7\ \times10^{-9}$	$1\ 9\times10^{-7}$	$2\ 2\times10^{-6}$
3 9			
West . .	$2\ 0\ \times10^{-9}$	$2\ 2\times10^{-7}$	$1\ 6\times10^{-6}$
East . . .	$1.8\ \times10^{-9}$	$2\ 0\times10^{-7}$	$1\ 6\times10^{-6}$
	Measured at 3 53 μ		
3 9			
West	$1\ 73\times10^{-8}$	$3\ 9\times10^{-7}$	$7\ 2\times10^{-7}$
East.......	$1\ 24\times10^{-8}$	$2\ 8\times10^{-7}$	$7\ 2\times10^{-7}$

value at $r \sim 3\,R_\odot$ and then decreases slowly. However, contrary to our earlier supposition, thermal radiation does not appear to be the dominant factor in coronal reddening, at least for $r < 3\,R_\odot$. It appears that we must again turn to diffraction for a complete interpretation of the reddening.

The present value of $R = 1.68$ at $2.5\,R_\odot$ tends, in effect, to confirm the large reddening measured by Blackwell (1952) of $R = 2.17$. At that time, Blackwell presented calculations with several dust-diffraction models in an attempt to interpret his reddening measurement. We have converted Blackwell's results into reddening coefficients for the three models. These are presented in the lower part of Figure 3 where they are normalized at $r = 1.5\,R_\odot$. The agreement between the observations and Blackwell's models, which assume a constant space density of single-sized dust particles, is not too good. It seems that no single-sized-particle model would reproduce the observed reddening. However, inclusion of a dust-density distribution can alter the reddening predicted by a diffraction model (Peterson 1967*b*).

Finally, Blackwell, Ingham, and Petford (1967) have presented a discussion in which they consider a decreasing dust density toward the Sun. Their model does not provide sufficient thermal reddening to explain either Blackwell's (1952) or the present reddening measurements. Even by allowing the albedo to decrease toward the Sun and the dust density to increase, their revised model predicts insufficient thermal radiation to account for the observations. Thus, some form of diffraction reddening seems to be required from a model of the interplanetary dust which is to explain successfully all the observable aspects of the F-corona. It seems unlikely that a dust model which successfully predicts very little color variation in the F-corona across the visible spectrum and also very little color variation in the zodiacal light (Peterson 1967*b*) can at the same time account for the amount of reddening observed with infrared coronal measurements. The present observations require a reddening which varies as $\lambda^{0.5}$. More calculations on dust models seem to be indicated.

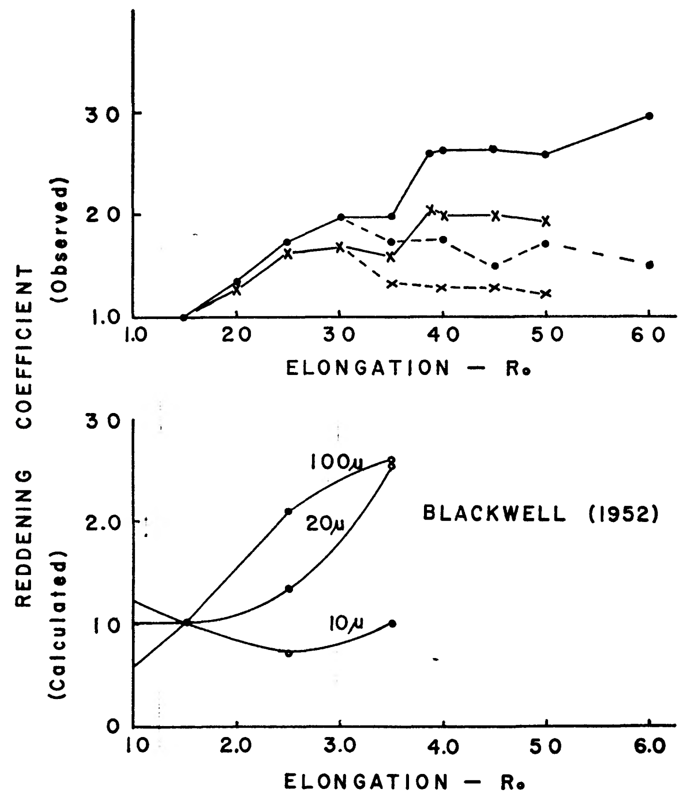

FIG. 3.—*Upper graph:* Observed reddening coefficients R as a function of elongation. Dots refer to west of Sun, crosses to east of the Sun. Contribution of thermal-emission reddening is apparent at $4\,R_\odot$. Dashed lines show reddening for $r > 3.5\,R_\odot$ when thermal reddening is removed; remainder is presumed to be due to diffraction reddening by the dust.

Lower graph: Theoretical values of the reddening coefficient based upon calculations by Blackwell.

IV. CONCLUSIONS

The eclipse measurements show conclusively, for the first time, the presence of thermal emission from interplanetary dust (Peterson and MacQueen 1967). Hence a new component, the thermal or T-component, has been added to the three recognized components of coronal radiation. The angular distribution of the thermal emission reveals particles moving in circular orbits and vaporizing completely as predicted by Peterson (1963). A second unexpected particle population apparently moving in elliptical orbits and not suffering complete vaporization is also indicated.

Our reddening coefficient for the range $1.5 < r < 2.5\,R_\odot$ has a value of 1.65 and tends to confirm Blackwell's (1952) value of 2.17. Thermal emission is found to contribute to the reddening coefficient for $r > 2\,R_\odot$ but apparently not for smaller elongations. The angular distribution of reddening, after removal of thermal-emission reddening, attains a maximum value of $R \sim 1.8$ at $r_2 = 3\, R_\odot$. No current dust model, which credibly reproduces the measurements of the zodiacal light, would seem to predict sufficient diffraction reddening to account for the observed coronal reddening.

With the present meager spectral information little can be said about the temperature of the dust when vaporization sets in; according to the calculation by Peterson (1963) the temperature would be $\sim 2000°$ K while Over's (1958) calculations on a SiO_2 dust model would indicate a temperature of $\sim 890°$ K when the dust is at $4\, R_\odot$. Our 3.5 μ measurement is consistent with the lower temperature. Only by examining the dust-emission spectrum for emission bands, if present, can one accurately define the temperature and the chemical composition of the interplanetary dust at each vaporization zone.

Infrared work at the University of Missouri was supported through a NASA Space Sciences Center sustaining grant. The eclipse expedition was financed by the Missouri University Research Council. Appreciation is expressed to Dr. Charles L. Hyder of Sacramento Peak Observatory and Professor Frank Q. Orrall of the University of Hawaii for allowing me to share their facilities at Huachacalla, Bolivia, and to Dr. H. S. Ahluwalia of the Laboratorio de Fisica Cosmica in La Paz for the many services provided.

REFERENCES

Allen, C. W. 1946, *M.N.R.A.S.*, **106**, 137.
Blackwell, D. E. 1952, *M.N.R.A.S.*, **112**, 652.
Blackwell, D. E., Ingham, M. F., and Petford, A. D. 1967, *M.N.R.A.S.*, **136**, 313.
Ingham, M. F. 1961, *M.N.R.A.S.*, **122**, 157.
Johnson, F. S. 1954, *J. Meteorol.*, **11**, 431.
MacQueen, R. M. 1967 (private communication).
Over, J. 1958, *Proc. Kon. Neder. Akad. v. Wetensch.*, **51B**, 74.
Peterson, A. W. 1963, *Ap. J.*, **138**, 1218.
———. 1964, presented at Cosmic Dust Symp., New York City, Nov. 21–22, 1963 and appearing in Ann. N.Y. Acad. Sci., **119**, 72.
———. 1967*a*, *Ap. J.* (*Letters*), **148**, L37.
———. 1967*b*, "The Zodiacal Light and the Interplanetary Medium," ed. J. L Weinberg, NASA Sp-150, p. 89.
Peterson, A W., and MacQueen, R. M. 1967, "The Zodiacal Light and the Interplanetary Medium," ed. J. L. Weinberg, NASA Sp-150, p. 89.